CENPD-285-NP-RAI
(NRC TAC No. M90188)

Fuel Rod Design Methods For Boiling Water Reactors: Response to Request for Additional Information

ABB Combustion Engineering Nuclear Operations

ABB

LEGAL NOTICE

CENPD-285-NP-RAI
(NRC TAC No. M90188)

Fuel Rod Design Methods for Boiling Water Reactors: Response to Request for Additional Information

July 1995

ABB Combustion Engineering Nuclear Operations

ABB

TABLES OF CONTENTS

This supplemental report contains responses to the NRC Requests for Additional Information regarding Reference A-12 which were transmitted to ABB by the NRC letter identified in Reference A-11.

Reference A-12 describes the ABB methods for fuel rod performance used for reload fuel rod design and safety analysis. Responses to the requests for additional information are provide here. The questions and responses are grouped into three categories.

- The first set designated with the prefix "A" relate to Section 1 through 3 of CENPD-285-P, describing the STAV6.2 fuel rod performance code.
- The second set designated with the prefix "B" relate to Section 4 and 5 of CENPD-285-P, describing the VIK-2 fuel rod mechanical analysis code.
- The third set designated with the prefix "C" relate to Section 6 through 7 of CENPD-285-P, describing the COLLAPS-II fuel rod creep collapse analysis code.

A. FINAL QUESTIONS ON CENPD-285-P, SECTIONS 1 TO 3 CONCERNING THE STAV6.2 FUEL ROD PERFORMANCE CODE

A.1 Questions and Responses

NRC Question A1

Are there any intended applications for the STAV6.2 code-not listed and demonstrated in the applications document, CENPD-287-P? In particular, are the intended burnup limits for STAV6.2 code application the same as those stated in CENPD-287-P? The stated limits are significantly greater than the bounding burnups for the data sets of fission gas release, cladding corrosion, cladding axial growth, and cladding creep. How can the application of these models be justified to the stated burnup limits when the models have not been verified to those burnups?

ABB Response to Question A1

The intended applications of the STAV6.2 code generally include the analyses described in Reference A-13 (CENPD-287-P) and the initial condition input to the transient analyses described in Reference A-24 (CENPD-300-P). The following table lists all of the parameters calculated by STAV6.2 and the document in which a description of the analysis is provided.

Parameter Calculated Using STAV6.2	Document in Which Calculation is Described
Fuel Rod Pressure	CENPD-287-P
Fuel Pellet Maximum Centerline Temperature	CENPD-287-P
Cladding Strain	CENPD-287-P
Clad Average Temperature for Cladding Collapse	CENPD-287-P
Cladding Stresses for Fatigue Analysis	CENPD-287-P
Gap Heat Transfer Coefficients for Fast Transients	CENPD-300-P
Gap Heat Transfer Coefficients for Loss of Coolant Accidents	CENPD-300-P
Gap Heat Transfer Coefficients for Control Rod Drop Accident Accidents	CENPD-300-P
Gap Heat Transfer Coefficients for Stability Analysis	CENPD-300-P

The intended burnup limits for the SVEA-96 BWR fuel assembly evaluations are stated in the Summary and Conclusions section of the applications document CENPD-287-P (Reference A-13). Specifically, these limits are a peak pellet burnup of [Proprietary Information Deleted]. The intended burnup limits for STAV6.2 code application are the same as those stated above. [Proprietary Information Deleted]

[Proprietary Information Deleted]

<u>NRC Question A2</u>

The code-to-data comparisons for fission gas release (Tables 3-8,3-9) are limited to cases where rod burnup does not exceed 45 GWd/MTU. We recommend comparisons be made to higher-burnup rods, particularly the BR-3 test rods described in Reference A-1, and the Riso test described in Reference A-2. If higher-burnup cases are not included, the code application for rod internal pressure will have to be limited to 45 GWd/MTU rod-average burnup.

<u>ABB Response to Question A2</u>

Code-to-data comparisons have been made to rods with an average burnup of up to [Proprietary Information Deleted]. These comparisons are described in the response to question A1.

In addition, comparisons between measured results in the BR-3 test rods and the Riso test rod have been made. These predictions were performed using the information provided in References A-1 and A-2 The results of these code comparisons are provided in Table A2-1.

[Proprietary Information Deleted]

<u>NRC Question A3</u>

Has the fission gas release model been compared to detailed post irradiation fuel examinations, where the partition between matrix-retained fission gas and gas stored in grain-boundary porosity has been measured, as a function of radial position in the pellet? [Such measurements have been reported, using combinations of electron microprobe radial scans with XRF scans (Reference A-3a) or microcoring (Reference A-3b)]. If so, please submit these comparisons. If not, discuss the consequences (for licensing applications) of errors in the estimate of this partition.

ABB Response to Question A3

[Proprietary Information Deleted]

NRC Question A4

The fission gas diffusion constants used by STAV6.2 for urania-gadolinia fuel are less than those used for urania-only fuel (Figure 2.1-7). Thus, urania-gadolinia rods may be predicted to release less gas than urania-only rods, even when the post-burnout temperature histories are similar. Please provide experimental evidence that specifically supports the difference in diffusion constants between the two fuel types, other than the integral comparison to fission gas release shown in Figure B-5?

ABB Response to Question A4

[Proprietary Information Deleted]

NRC Question A5

What are the functional forms and values for the parameters b(t) and "lambda" in the thermal fission gas release model? What are the bases for the choices that have been made?

ABB Response to Question A5

In the thermal fission gas release model in STAV6.2 the parameter b is the re-solution probability of gas atoms from intergranular bubbles (s^{-1}), while the parameter λ is the re-solution layer depth from intergranular bubbles. These parameters were introduced in Reference A-16 (Speight) for describing the migration of fission product gases in UO_2 fuel. Reference A-19 (White and Tucker) note that the value of λ is < 0.01 μm and they reason that b is of the order of 2×10^{-5} s^{-1} for a fission rate ~10^{19} m^{-3} s^{-1} and a bubble radius of ~0.001 μm. Therefore, the value of the composite parameter $b\lambda$ is in the region of 10^{-13} m/s.

As noted in Reference A-19 (White and Tucker) one would expect the value of $b\lambda$ to be dependent on fission rate. Since power density is a measure of fission rate the functional form of $b\lambda$ can be expressed as:

$$b\lambda = (b\lambda)_o Q/Q_o$$

where Q is the power density (W/kg) and the index o indicates a reference state.

In STAV6.2, we assume that the ratio $b(t)/\beta(t)$ (where $\beta(t)$ is the rate of fission gas generation) is time independent since both b and β are proportional to the fission rate. [Proprietary Information Deleted]

NRC Question A6

Please plot the fission gas release predictions from the thermal fission gas release model described in Section 2.1.5.2 of Reference A-12 for a single ring of fuel at fixed temperature, as a function of burnup. Plot the release vs. burnup from 0 to 70 GWd/MTU, for a series of (constant) temperatures, beginning with 800°C and ascending in 200°C increments to 2000°C. State the major assumptions made in these calculations: e.g., the external pressure (P_{ext} in equation 2.1-34 in Reference A-l); the surface tension; the nominal bubble radius and dihedral angle; the fractional areal coverage (of grain surface) corresponding to saturation; and the assumed grain radius. Indicate the connection between these assumed parameters and the values or functions typically used within the STAV6.2 code.

ABB Response to Question A6

In STAV6.2, the fission gas release is composed of two components: athermal release and thermal release.

Calculations of the thermal fission gas release have been performed with the ABB model [Proprietary Information Deleted] Calculations have been performed using the parameters shown in Table A6-1. The parameters were chosen so that the effect of the burnup and temperature on fission gas release would be evident. The calculation is not intended to represent a typical design calculation because the ABB fuel designs generally experience very little thermal fission gas release. The relationship of each of the parameters chosen to the values normally used in STAV6.2 is provided in Table A6-1 under description. [Proprietary Information Deleted]

NRC Question A7

The RADAR subroutine used in STAV6.2 to generate burnup-dependent radial power distributions has a fixed-form for distribution of plutonium within the pellet. As a consequence, the calculated width of the region with ultra high burnup and high volumetric heat generation remains constant with increasing burnup. However, electron microprobe scans across transverse fuel cross sections in PIE indicate that the width of the high-burnup, high-power rim region increases with burnup (see for example, Reference A-3a). Furthermore, the radial peak (edge-peak) values of the radial power distribution are underestimated by the original

RADAR since it fails to account for the plutonium isotopes explicitly (see Lassmann, 1994, Reference A-4). What are the estimated consequences of these deficiencies to calculated fuel temperatures?

ABB Response to Question A7

The RADAR subroutine used in STAV6.2 generates a radial power distribution within the fuel pellet which results in a radial burnup distribution within the pellet. When the radial burnup distribution is normalized to the pellet average burnup, the shape of the resulting curve is nearly independent of pellet average burnup. However, the shape does exhibit a sharp increase in local burnup near the surface of the pellet. [Proprietary Information Deleted]

[Proprietary Information Deleted]

NRC Question A8

The formulation of the radial heat transfer solution does not imply any burnup-dependent degradation of the fuel thermal conductivity. However significant degradation is proposed by Kolstad et al. of the Halden Project (Reference A-5), based on in-reactor fuel temperature measurements. Note that the data base for Halden's assertion includes Rod 3 of Assembly IFA-432. The trend is corroborated by measurements on SIMFUEL (simulated burned-urania fuel) by Lucuta (Reference A-6). Is the fuel thermal conductivity in STAV6.2 a function of temperature only, or is it also a function of burnup? If it is not a function of burnup, please explain why it is not.

ABB Response to Question A8

The fuel thermal conductivity model in STAV6.2 is a function of temperature only, and is not a function of burnup. When the code was under development, it was recognized that fuel pellet thermal conductivity might be degraded slightly with increasing burnup, but experimental data was not available to support the inclusion of a burnup effect into the thermal conductivity model. [Proprietary Information Deleted]

[Proprietary Information Deleted]

NRC Question A9

The calculated fuel thermal conductivity in STAV6.2 at high temperatures (> 2000°C) is significantly higher than normally accepted values (e.g., References 7 and 8). This is a consequence of holding the phonon term constant for temperatures greater than a certain value. Please state the justification for the STAV6.2 high-

temperature fuel thermal conductivity values and what is the impact on calculated fuel melting?

ABB Response to Question A9

[Proprietary Information Deleted]

NRC Question A10

Is the fuel thermal conductivity modified by a "crack factor" related to added thermal resistance due to fuel pellet cracking? Or, is crack porosity and relocated gap volume included in the porosity correction factor for the thermal conductivity? Or, is no account taken of crack-related reduction in fuel thermal conductivity?

ABB Response to Question A10

[Proprietary Information Deleted]

NRC Question A11

Based on Figure 2.1.2 of CENPD-285-P, the STAV6.2 fuel volumetric swelling rate is significantly smaller than the commonly used value of 1.0% per 10 GWd/MTU. The commonly-used value is corroborated by recent hot cell examinations of extended-burnup C-E fuel (Reference A-9) and other examinations (Reference A-10). Please justify the smaller swelling rate used in STAV6.2.

ABB Response to Question A11

[Proprietary Information Deleted]

NRC Question A12

Please provide STAV6.2 detailed output information from two licensing calculations for the ABB BWR design, one for the maximum end-of-life fission gas release, and one for peak fuel temperature. Include the normal code input data for these cases, the linear heat generation rates and the axial power profiles at each time step. At intervals not to exceed 5 GWd/MTU, please provide the axial peak node position and LHGR, the current fission gas release and fill gas composition, and the peaknode radial temperature distribution throughout the fuel pellet and cladding. The peak node hot gap size at each time step is also requested.

ABB Response to Question A12

The ABB methodology for verifying the acceptability of a fuel rod design for a particular plant application, which is described in

Reference A-13 (CENPD-287-P), does not include a specific calculation of the fission gas release (FGR) at the end of life (EOL). However, the EOL FGR can be conservatively estimated using the methodology for calculating the EOL rod pressure.

The EOL rod pressure calculation is performed by [Proprietary Information Deleted]

Dimensional inputs to the calculation performed for the Staff's review are shown in Table A12-1. [Proprietary Information Deleted] The power history and axial power shapes are provided in Table A12-2 and A12-3, respectively.

Results of the calculations are shown in Tables A12-4 through A12-6. In addition, the data is also plotted in Figures A12-1 through A12-5.

NRC Question A13

Why is the volume of the fuel-cladding gap excluded from the list of volumes considered for pressure calculations (Table 2.3-1)? What is the estimated effect of this omission?

ABB Response to Question A13

The volume of fuel-pellet cladding gap is accounted for in rod pressure calculations. m This was an error in the word processing. Table 2.3-1 should read:

TABLE 2.3-1

PROPRIETARY INFORMATION DELETED

NRC Question A14

What effect might gamma heating of plenum region cladding and the end pellet and the plenum spring have on the plenum gas temperature? Can the plenum gas really be considered to have exactly the local coolant temperature, as is apparently assumed in the STAV6.2 code? Does ABB have evidence to support this estimate of the plenum temperature? What is the impact on rod gas pressures if the plenum is assumed to be 10°C higher?

ABB Response to Question A14

[Proprietary Information Deleted]

NRC Question A15

The source of BWR creep data is an irradiation test in the R2 reactor at Studsvik that is neither described nor referenced. Please describe this test, including:

Cladding materials involved.

Operating conditions (temperatures, pressures and stresses, flux levels).

Design features of the test assemblies pertinent to creep results.

Also please indicate which data points in Figures 3.43 to 3.49 of CENPD285-P are from the BWR test and which are PWR data. Are the BWR data limited to the very low strain rates?

ABB Response to Question A15

[Proprietary Information Deleted]

NRC Question A16

Why is it necessary (and why is it appropriate) to compare the BWR (Zircaloy-2) model against unfuelled PWR (Zircaloy-4) [Franklin, Lucas, Bement] tube data from the Oconee reactor? Are there no appropriate high-fluence, BWR cladding creep data to compare the BWR model against? Is the metallurgical condition of the Oconee tubes sufficiently similar to that of the BWR cladding types to justify comparison to the BWR creep model?

ABB Response to Question A16

[Proprietary Information Deleted]

NRC Question A17

The cladding creep models are stated to be derived from Nichols (reference 2-15). From our reading of reference 2-15, we cannot make a direct connection. Was the Nichols paper used only for general guidance, or was there an actual mathematical derivation of the STAV-6.2 models from the more general (and more complex) Nichols formulation? If so, how was it done?

ABB Response to Question A17

[Proprietary Information Deleted]

NRC Question A18

The comment is made on page 51 that "Due to the increase of the yield strength with neutron fluence, a large number of PCMI cases do not result in cladding yielding". What is the yield strength as a function of fluence at high fluence (> 1×10^{26} n/m2), and what is its basis? Is the yield strength also considered as a function of cladding hydrogen content?

ABB Response to Question A18

[Proprietary Information Deleted]

NRC Question A19

The formation of a "rim structure" in the ultra-high burnup rim of high burnup fuel pellets is well known (Reference A-3). This rim structure is characterized by a very high concentration of fission products and enhanced small porosity accumulating on the boundaries of sub-grains that are typically < 1 micron in diameter. The possibility exists for enhanced fission gas release and highly degraded fuel thermal conductivity in this region. Are any rim structure effects accounted for in the STAV6.2 code? If not, please justify these omissions.

ABB Response to Question A19

[Proprietary Information Deleted]

NRC Question A20

What is the burnup range represented by the "beginning of life" (BOL) data set for fuel center temperatures? Please add IFA-513 rods 1 and 2 and IFA-432 Rods 1 and 5 to the BOL data base for fuel centerline temperatures. Then, tabulate the code-data comparisons on fuel centerline temperature vs. rod-average burnup (at increments not greater than 2 GWd/MTU) for the following: IFA-432, Rods 1,2, 3, and 5; and IFA-513, Rods 1,2, and 6. Extend these seven tables to include all available data; i.e., show the comparisons to both upper and lower thermocouple data, out to the maximum burnup for which data is reported in open-literature publications.

ABB Response to Question A20

[Proprietary Information Deleted]

Beginning of life STAV6.2 predictions of pellet centerline temperature have been performed for IFA-432 Rods 1 and 2 and IFA-

513 rods 1 and 5. The code to data comparisons are presented in Figures A20-1 through A20-4 and Tables A20-1 through A20-4. [Proprietary Information Deleted]

[Proprietary Information Deleted]

NRC Question A21

Do the rods listed in Table 3-11 (corrosion data) have the beta-quenched type cladding? If not what is the maximum exposure level for corrosion data from the beta-quenched type cladding?

ABB Response to Question A21

The rods listed in Table 3-11 of Reference A-12 (corrosion data) are [Proprietary Information Deleted]

[Proprietary Information Deleted]

A.2 References

A-1 Balfour, M. G., et al. 1982. BR-3 High Burnup Fuel Rod Hot Cell Program Vol. 1: Final Report, DOE/ET/34073-1, WCAP-10283.

A-2 Bagger, C., et al. 1978. In-Pile Determination of UO_2 Thermal Conductivity Density Effects and Gap Conductance, for the Danish UO_2-Zr Irradiation Test 022, RISO-M-2152.

A-3a Barner J. O., et al. 1993. "Evaluation of Fission Gas Release in High-Burnup Light Water Reactor Fuel Rods", Nuclear Technology Vol. 102, pp. 210-230.

A-3b Manzel, R. 1991. "Fission Gas Release at High Burnup and the Influence of the Pellet Rim", International ANS/ENS Topical Meeting on LWR Fuel Performance Avignon. France, p. 528.

A-4 Lassmann, K. 1994. "The Radial Distribution of Plutonium in High Burnup UO_2 Fuels", Journal of Nuclear Materials 208, pp. 223-231.

A-5 Kolstad, E., 1991. "Fuel Rod and Core Materials Investigations Related to LWR Extended Burnup Operation", Journal of Nuclear Materials, Vol. 188, pp. 104-113.

A-6 Lucuta, P. 1991. "Thermal Conductivity of SIMFUEL", Journal of Nuclear Materials Vol. 188, pp. 198-204.

A-7 Lyons., M. F., et al. 1964. UO_2 Pellet Thermal Conductivity from Irradiations to Central Meeting. GEAP-4624.

A-8 Hagrman, D. L., et al. eds. 1981. MATPRO-Version 11 (Revision 2: A Handbook of Materials Properties for Use in the Analysis of Light Water Reactor Fuel Rod Behavior. NUREG/CR-0479, TREE-1280, Rev. 2.

A-9 G.P. Smith Jr., et al. 1993. Hot Cell Examination of Extended Fuel from Calvert Cliffs-1, EPRI Report TR-103302, Project 2905-02 Final Report.

A-10 Stehle, H. 1976. "In-Reactor UO_2 Densification", Journal of Nuclear Materials 61, p. 326

A-11 S. Wu (NRC) to D. Ebeling-Koning (ABB CENO) Letter, "Request for Additional Information on CENPD-285-P, 'Fuel Rod Design Methods for Boiling Water Reactors' (TAC No. M90188)," February 7, 1995.

A-12 Fuel Rod Design Methods for Boiling Water Reactors, ABB Report CENPD-285-P (1994).

A-13 Fuel Assembly Mechanical Design Methodology for Boiling Water Reactors, ABB Report CENPD-287-P (1994).

A-14 Pati, S.R., Garde, A.M., and Clink, L.J., Contribution of Pellet Rim Porosity to Low-Temperature Fission Gas Release at Extended Burnups, ANS Topical Meeting on Light Water Reactor Fuel Performance, April 17-20, 1988, Williamsburg, VA.

A-15 D G Franklin, G E Lucas and A L Bement, *Creep of Zirconium Alloys in Nuclear Reactors*, ASTM Publication (STP 815), Philadelphia, (1983).

A-16 Speight, M. V., "A Calculation of the Migration of Fission Gas in Material Exhibiting Precipitation and Re-solution of Gas Atoms under Irradiation", Nucl. Sci. Eng., Vol. 37, pp 180-5 (1969).

A-17 B Grapengiesser et al, Proceedings of Symposium on Improvements in Water Reactor Fuel Technology and Utilization, Stockholm, 15-19 September 1986, pp 281-289. IAEA publications, Vienna (1987).

A-18 B. Grapengiesser et al, Proceedings of ANS Topical Meeting on LWR Fuel Performance, April 17-29, 1988, Williamsburg, Virginia, pp 31-40 (1988).

A-19 R.J. White and M.O. Tucker, A New Fission Gas Release Model, *J. Nucl. Mater.* 118,1-38 (1983).

A-20 Hagrman D L, et al, MATPRO-Version 11: A Handbook of Material Properties for Use in the Analysis of Light Water Reactor Fuel Rod Behavior, NUREG/CR-0497, TREE-1280, (1979).

A-21 Yasuda, T., Nakatsuka, M., and Yamashita, K., "Deformation and Fracture Properties of Neutron-Irradiated Recrystallized Zircaloy-2 Cladding under Uniaxial Tension," Zirconium in the Nuclear Industry: Seventh International Symposium, ASTM STP 939, R. B. Adamson and L. F. P. Van Swam, Eds., American Society for Testing and Materials, Philadelphia, 1987, pp. 734-747.

A-22 Smith, P. G., Pirek, R. C., and Griffiths, M., "Hot Cell Examination of Extended Burnup Fuel from Calvert Cliffs-1", EPRI TR-103302-V2, Project RP2905-02 Final Report Vol. 2 (May 1994).

A-23 Smith, G. P., Pirek, R. C., Freeburn, H. R., and Schrire, D., "The Evaluation and Demonstration of Methods for Improved Nuclear Fuel Utilization", DOE/ET/34013-15, Final Report (August 1994).

A-24 Reference Safety Report for Boiling Water Reactors, ABB Report CENPD-300-P, November, 1994.

A-25 M. R. Smith, W. Wiesenack, H. Devold, "A Review of Halden Tests and Measurements Relating to Fuel Thermal Properties," HWR-302, May, 1991.

TABLE A1-1 STAV6.2 CALIBRATION OF FUEL PERFORMANCE DATA

PROPRIETARY INFORMATION DELETED

TABLE A2-1 RESULTS OF STAV6.2 FISSION GAS RELEASE AND ROD VOID PREDICTIONS OF RISO AND BR-3 TEST RODS

PROPRIETARY INFORMATION DELETED

TABLE A6-1 INPUTS USED IN CALCULATION OF THERMAL FISSION GAS RELEASE

PROPRIETARY INFORMATION DELETED

TABLE A6-2 TIME AND BURNUP FOR FIRST THERMAL FISSION GAS RELEASE

PROPRIETARY INFORMATION DELETED

TABLE A6-3 TOTAL THERMAL FISSION GAS RELEASE

PROPRIETARY INFORMATION DELETED

TABLE A9-1 FUEL PELLET THERMAL CONDUCTIVITY MODELS

PROPRIETARY INFORMATION DELETED

TABLES A12-1 THROUGH A12-6

PROPRIETARY INFORMATION DELETED

TABLE A15-1 S268/S269 FUEL ROD DESIGN

PROPRIETARY INFORMATION DELETED

TABLE A15-2 S268/S269 MEASURED AND PREDICTED CREEP STRAIN

PROPRIETARY INFORMATION DELETED

TABLE A17-1 ZIRCALOY CREEP MECHANISMS

PROPRIETARY INFORMATION DELETED

TABLE A20-1 THROUGH A20-11

PROPRIETARY INFORMATION DELETED

Figure A1-1 through A1-4
Proprietary Information Deleted

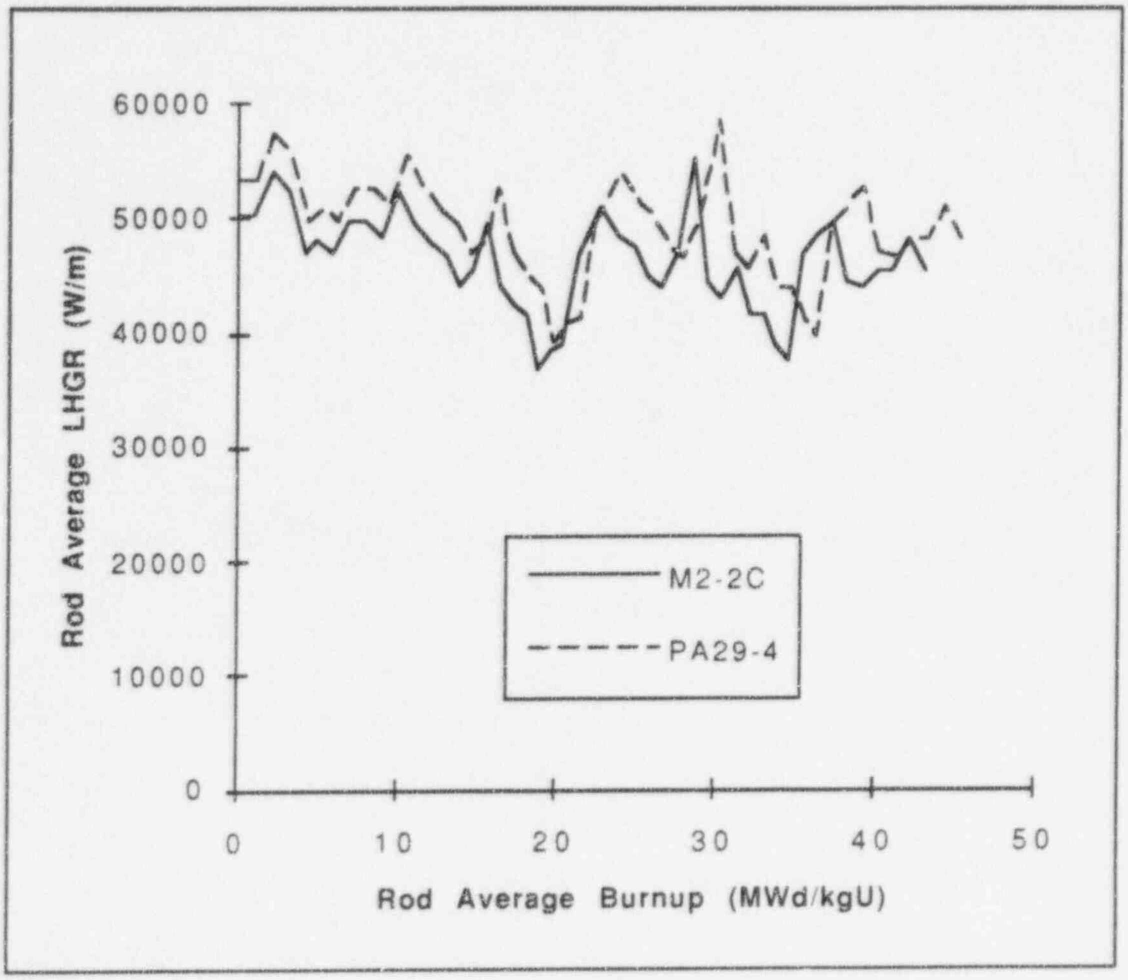

Figure A2-1 RISO Rods PA29-4 and M2-2C Power Histories

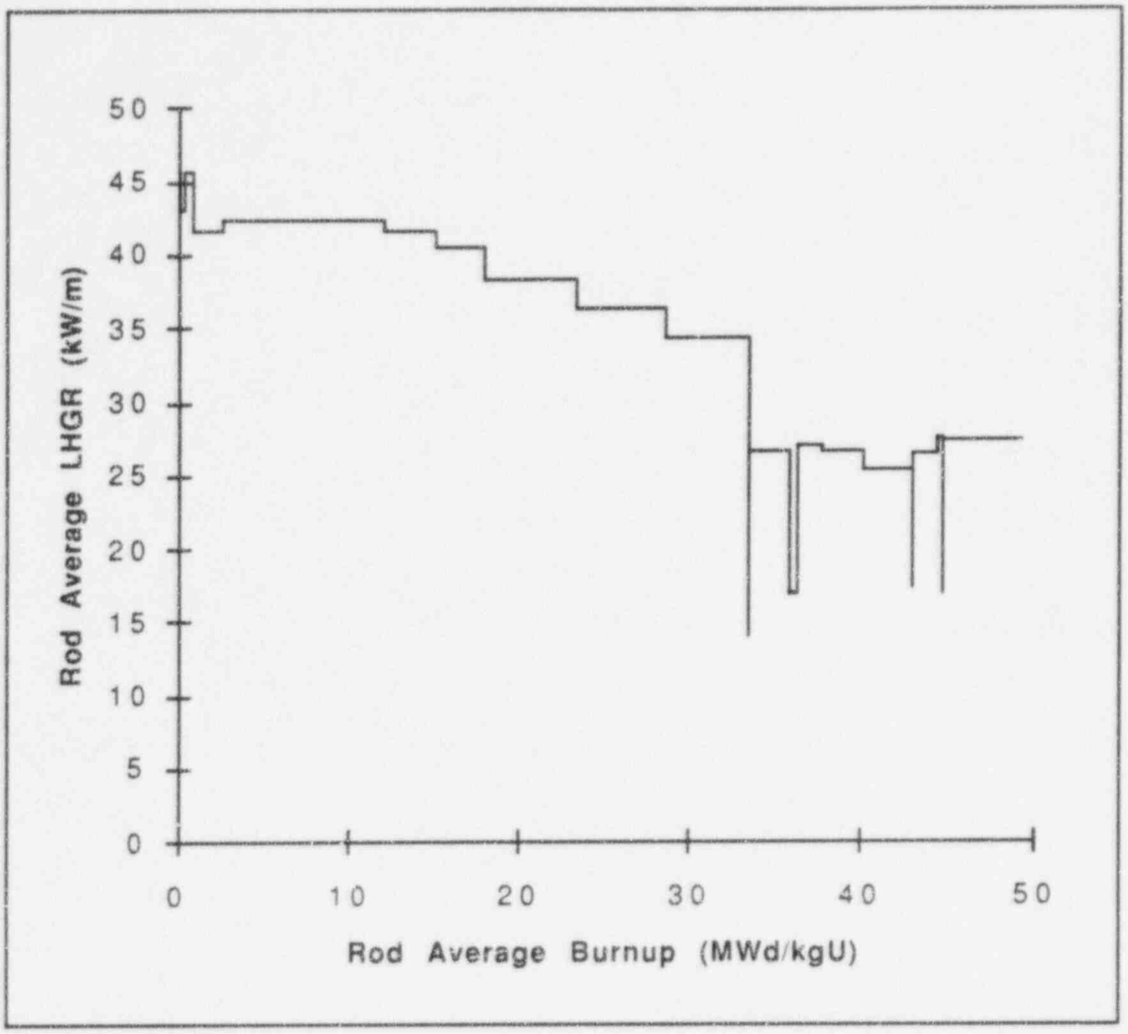

Figure A2-2 BR-3 Rod 111I5 Power History

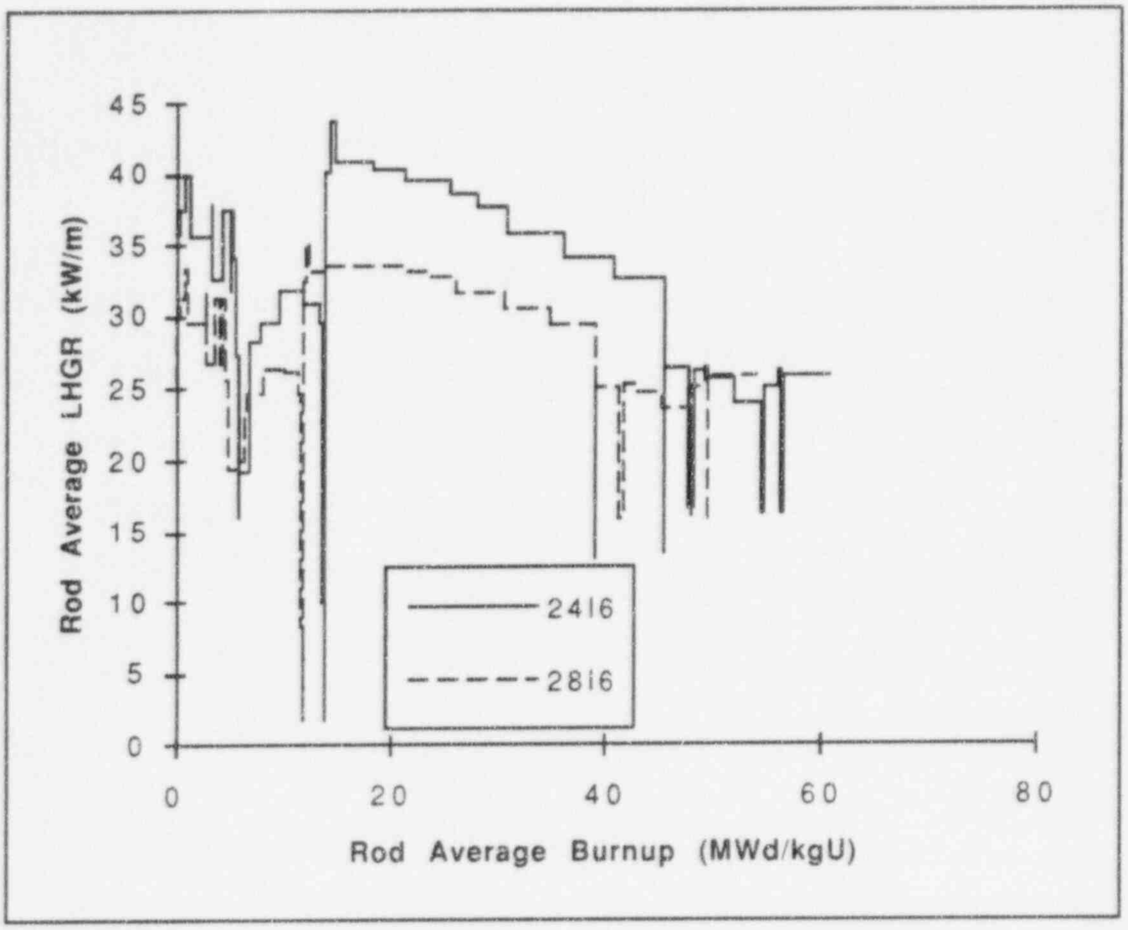

Figure A2-3 BR-3 Rods 24I6 and 24I8 Power Histories

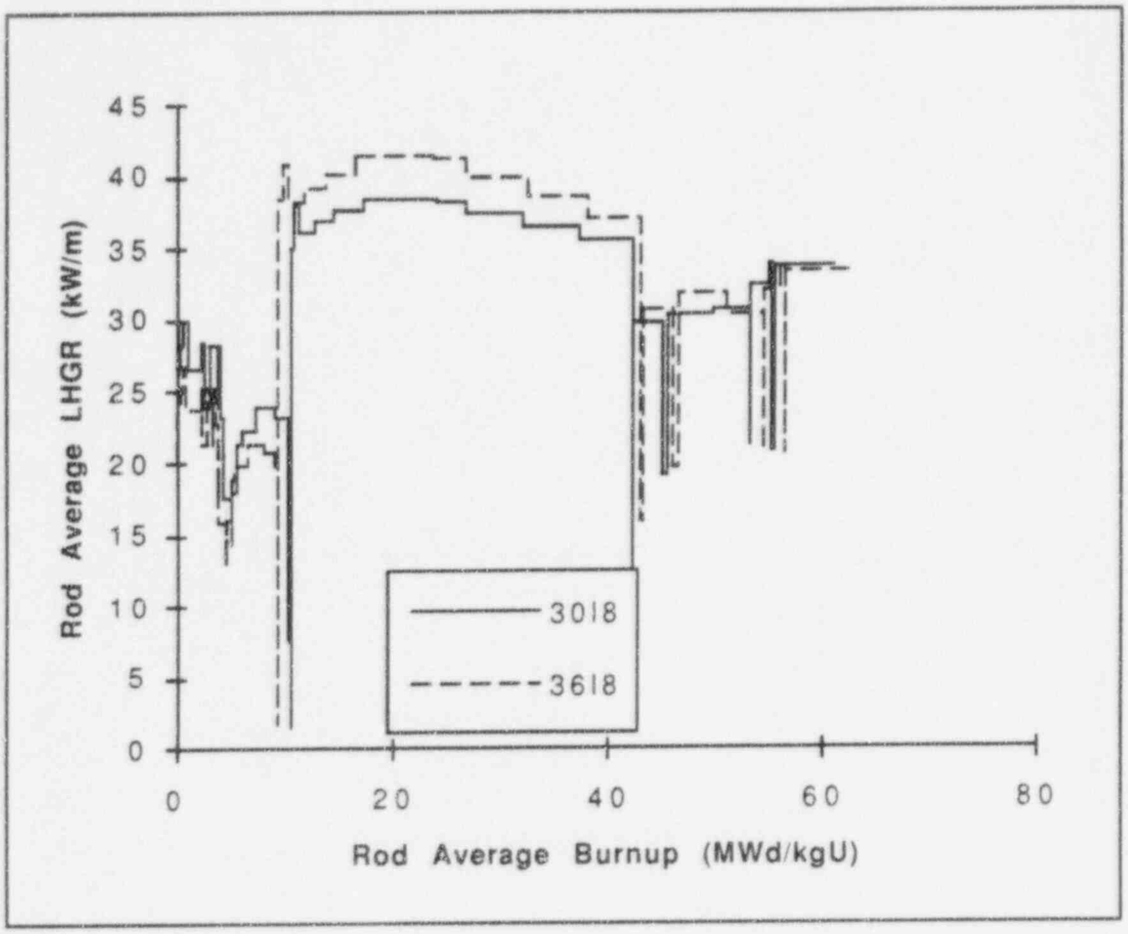

Figure A2-4 BR-3 Rods 30I8 and 36I8 Power Histories

Figure A4-1 Proprietary Information Deleted

Figure A6-1 & A6-2 Proprietary Information Deleted

Figure A12-1 through A12-5 Proprietary Information Deleted

Figure A20-1 through A20-7 Proprietary Information Deleted

B. FINAL QUESTIONS ON CENPD-285-P, SECTIONS 4 AND 5 CONCERNING THE VIK-2 FUEL ROD MECHANICAL ANALYSIS CODE

NRC Question B1

Poisson's Ratio in Equation 4.1-7 should be raised to the third power, not to the second power. Does this error propagate to other derivations, and is it present in the FORTRAN coding?

ABB Response to Question B1

The correct value for the exponent for the Poisson's ratio in Equation 4.1-7 is 2. The reference on which Equation 4.1-7 was based has a typographical error. This error was discovered prior to the development of the VIK–2 code and the correct value was used in the code. For your review is the derivation of the flexural rigidity of a plate or shell.

Consider a plate with thickness h, which in a nonloaded condition occupies the region $-\frac{h}{2} \le z \le \frac{h}{2}$ in a coordinate system (x,y,z). We can study the motion of a point P in the plate as it deforms, see figure below. We denote by w the vertical displacement of a point in the neutral surface, i.e., its z coordinate

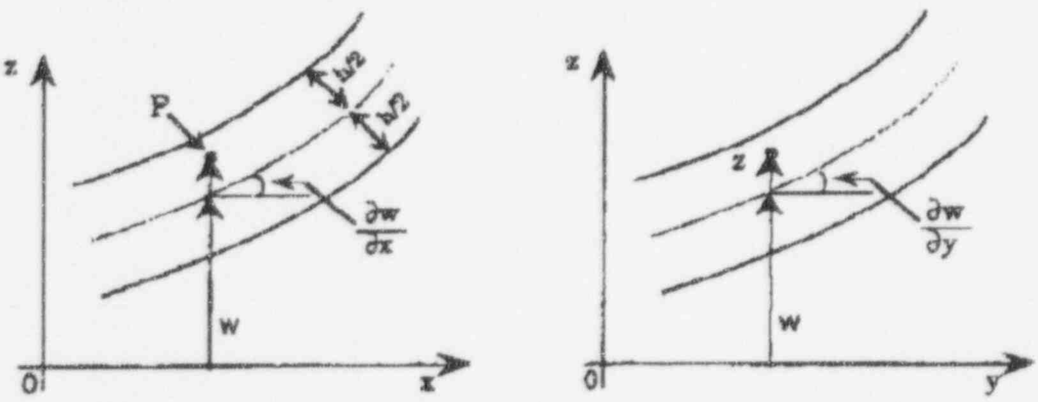

Under deformation the displacements of point P in the x and y directions are

$$u = -z\frac{\partial w}{\partial x} \qquad v = -z\frac{\partial w}{\partial y}$$

The associated strain components are:

$$\varepsilon_x = -z\frac{\partial^2 w}{\partial x^2},\ \varepsilon_y = -z\frac{\partial^2 w}{\partial y^2},\ \varepsilon_{xy} = -2z\frac{\partial^2 w}{\partial x \partial y}$$

For thin plate $\sigma_x = 0$. Using Hooke's law for linearly elastic material gives:

$$\sigma_x = \frac{Ez}{1-\upsilon^2}\left(\frac{\partial^2 w}{\partial x^2} + \upsilon\frac{\partial^2 w}{\partial y^2}\right)$$

$$\sigma_y = \frac{Ez}{1-\upsilon^2}\left(\frac{\partial^2 w}{\partial y^2} + \upsilon\frac{\partial^2 w}{\partial x^2}\right)$$

$$\sigma_{xy} = \frac{Ez}{(1+\upsilon)}\ \frac{\partial^2 w}{\partial x \partial y}$$

where E is Young's modulus and υ is Poisson's ratio. The results of these stresses per unit length along the neutral line are denoted by M_x, M_y, and M_{xy} respectively:

$$M_x = \int_{-h/2}^{h/2} \sigma_x z dz = \int_{-h/2}^{h/2} \frac{Ez^2}{1-\upsilon^2}\left(\frac{\partial^2 w}{\partial x^2} + \upsilon\frac{\partial^2 w}{\partial y^2}\right)dz$$

$$= -D\left(\frac{\partial^2 w}{\partial x^2} + \upsilon\frac{\partial^2 w}{\partial y^2}\right)$$

where

$$D = \frac{Eh^3}{12(1-\upsilon^2)}$$

D is called the *flexural rigidity* of the plate.

Similarly,

$$M_y = \int_{-h/2}^{h/2} \sigma_y z dz = -D\left(\frac{\partial^2 w}{\partial y^2} + \upsilon\frac{\partial^2 w}{\partial x^2}\right)$$

$$M_{xy} = \int_{-h/2}^{h/2} \sigma_{xy} z dz = -D(1-\upsilon)\frac{\partial^2 w}{\partial x \partial y}$$

C. FINAL QUESTIONS ON CENPD-285-P, SECTIONS 6 AND 7 CONCERNING THE COLLAPS-II CREEP COLLAPSE ANALYSIS CODE

C.1 Questions and Responses

NRC Question C1

Page 229. Zircaloy cladding tubing is well-known to be anisotropic microstructurally, and to behave anisotropically in both elastic and plastic deformation. Discuss the acceptability of the isotropic assumption for this application.

ABB Response to Question C1

[Proprietary Information Deleted]

NRC Question C2

Equation 6.1-4 appears to be identical to Dieter's plane stress formulation (Reference 1, equation 2.77) rather than that of plane strain. Please explain.

ABB Response to Question C2

Equation 2-64 of Reference C-4 (Reference 1 in question) is a statement of the relationship between stress and strain for an elastic solid. It is, therefore, a statement of Hooke's Law, where E is the Young's Modulus of the solid. Equation 6.1-3a of Reference C-2 is a generalized but also a statement of Hooke's Law, where D is the flexural rigidity of a shell.

Equations 2-77 of Reference C-4 can be derived directly from Equation 2-64 of Reference C-4 if σ_3 is set to zero. This is referred to as "plane stress" and applies to an elastic solid.

The expansion of the generalized stress-strain relation, equation 6.1-3a of Reference C-2, and application of the assumption that the radial stress (σ_r) is zero, the resulting equations Equation 6.1-4 apply to an elemental shell segment and have the same form as those in equation 2-77 of Reference C-4. Both equations 6.1-4 of Reference C-2 and 2-77 of Reference C-4 are formulations of Hooke's Law with one component of stress set to zero. The assumption that the radial stress is zero, applies throughout the development of the shell equations that define the behavior of the shell. The radial stress does not appear in the stress resultant equations (6.1-6) nor in the equilibrium equations.. For example, see Section 2.2 and subsequent sections of Reference C-5 where this assumption is among several that are basic to the formulation of their shell equations.

The assumption that $\sigma_r = 0$ leads to a relationship between the strains ε_r, ε_θ, and ε_z (see equation 6.1-4d of Reference C-5). However, the assumption of generalized plane strain is applied in Paragraph 6.1.2 of Reference C-2 based on the physical characteristics of a fuel tube as having a very long length relative to its diameter and thickness and is not directly related to the formulation of Hooke's Law with $\sigma_r=0$. The generalized plane strain assumption is valid because the shell (fuel tube) in question is very long, therefore the strain in the Z direction does not vary around the circumference of the cylinder. It is not necessarily zero or negligible but simply constant around the circumference.

This assumption, which is common in cylindrical shell theory, allows the problem to be reduced to that of a shell of unit width, by removing a "slice" from the shell and simulating the axial effect with the appropriate strain condition.

NRC Question C3

Page 234. Do the results of the calculation depend on which moment (M_2 or M_A) is chosen for evaluation? Could load shedding occur during the incremental computation (i.e., from the high load region to the low load region) that would lengthen the calculated collapse time?

ABB Response to Question C3

[Proprietary Information Deleted]

NRC Question C4

Page 266: The assumption of plane strain leads to a fictitious axial force. Does this in turn stiffen the tubing mathematically, thus increasing the calculated time-to-collapse? Discuss the probable consequences of a plane-stress formulation of this solution.

ABB Response to Question C4

In the development of Equation 2-78, Reference C-4 states that plane strain occurs "when one dimension is much greater than the other two, as in a long rod or cylinder with restrained ends." A fuel tube is a long cylinder with unrestrained ends and a net axial force resulting from the net pressure on the end area.

[Proprietary Information Deleted]

NRC Question C5

Please compare COLLAPS-II to actual creep collapse data (drawn from CEPAN OR BUCKLE reference lists or other sources), including a range of ovalities, differential pressures, and temperatures that bracket the intended applications, if possible.

ABB Response to Question C5

[Proprietary Information Deleted]

NRC Question C6

What is considered to be the root cause of the fact that COLLAPS-II predicts longer times-to-collapse than either CEPAN or BUCKLE

ABB Response to Question C6

[Proprietary Information Deleted]

C.2 References

C-1 P. J. Pankaskie, An Analytical Computer Code for Calculating Creep Buckling of an Initially Oval Tube, Battelle Pacific Northwest Laboratories Report, BNWL-1784, (1974).

C-2 Fuel Rod Design Methods for Boiling Water Reactors, ABB Report CENPD-285-P (1994).

C-3 R. Hill, The Mathematical Theory of Plasticity, Oxford Press, 1956.

C-4 George E. Dieter, "Mechanical Metallurgy," Second Edition, McGraw-Hill Book Co.

C-5 H. Kraus, "Thin Elastic Shells", John Wiley & Sons, Inc., 1967.

TABLE C5-1 COMPARISON OF CALCULATED AND MEASURED OVALITIES

PROPRIETARY INFORMATION DELETED

Figure C5-1 Predicted versus Measured Ovality
Proprietary Information Deleted

ABB

ABB Combustion Engineering Nuclear Operations
Combustion Engineering, Inc.
1000 Prospect Hill Road
Post Office Box 500
Windsor, Connecticut 06095-0500